Mass distribution in quadruple gravitational lenses

B. Mihov, L. Slavcheva-Mihova
Institute of Astronomy and NAO, Bulgarian Academy of Sciences

Abstract. Strong gravitational lensing provides us with an independent method to study the matter distribution in galaxies, acting as lenses, irrespective of the mass nature. The number and accuracy of the observational constraints are of importance for building reliable lens mass models.
We select a sample of quadruple lens systems with available time delay estimates to increase the number of the observational constraints. The most precise values of the time delays (e.g., obtained in the course of COSMOGRAIL programme), positions (for some of the lensed systems we derived improved positional constraints using HST imaging), and redshifts are compiled. The HST light distribution of the lenses is decomposed using the GALFIT package. The individual mass profiles are determined on the basis of non-parametric modeling and analysed in the framework of various parametric dark matter models. In addition, we compare and discuss the mass and light distribution of the sample lenses.

1. Introduction

The strong gravitational lensing provides us with an independent method to study the matter distribution in galaxy-lenses irrespective of the mass nature. The number and accuracy of the observational constraints are of importance for building reliable lens mass models.

We present (i) a non-parametric lens mass reconstruction of lensed systems with the aim to obtain estimates of the slope of the lens mass profiles and (ii) a parametric light distribution modeling to get the geometric parameters of the main galaxy-lens. For this study we selected three quadruple lenses (DES J0408–5354, PG 1115+080, and WFI 2033–4723) for which precise estimate of the time delay exists.

2 Mass and Light Modeling

The non-parametric mass modeling was done by means of PixeLens software (version 2.17, Saha & Williams 2004). The mass models were chosen to be symmetric with *pixrad* parameter of 10. Given the mass map radius in arcsec, this parameter sets the scale of the map in arcsec/px. In case of a companion galaxy to the main lens, we added a point mass to the model. The maximal allowed area, covered by the point mass Einstein radius, is assumed to be 15 arcsec^2, which is a reasonable value for galaxy scale lenses. We ran 100 models for each lens.

The light distribution modeling was done with GALFIT software (version 3.0.5, Peng et al. 2010) that allows accounting for asymmetric structures if present. We fit simultaneously the galaxy-lens and the lensed images. The PSF used to model the quasar images and to convolve the galaxy model was constructed using the Tiny Tim software.

3 Results

DES J0408–5354. This quad was found by Lin et al. (2017) in the course of the Dark Energy Survey. They measured redshifts of the source and lens z_S = 2.375 and z_L = 0.597, respectively. The strometry is taken from Shajib et al. (2019). Image C is strongly dimmed by a foreground galaxy with position very close to that of the image in this system. By reason of this the time delays, estimated by Donnan et al. (2021), do not include image C. The galaxy G2 (Lin et al. 2017), which is very close to image C was modeled by a point mass, offset by 0.3 arcsec to the East. We found dt(BC) = 7.0 (+1.0/–1.2) d and dt(CD) = 16.0 (+4.7/–7.3) d at 68% confidence. Using the relation dt(i,k) = dt(i,j) + dt(j,k), we can see that our estimates agree to within the uncertainties with the dt(AD) and dt(BD) delays as measured by Donnan et al. (2021): dt(AD) = –159.1 (+1.8/–1.7) d and dt(BD) = –47.6 (+1.3/–1.4) d.

PG 1115+080. This quad is the second lensed quasar discovered (Weymann et al. 1980, z_S = 1.722). The redshift of the galaxy, z_L = 0.3098, is taken from Tonry et al. (1998). The most recent astrometry, based on the HST observations, was presented by Morgan et al. (2008). The time delays in the system were determined by several groups, but the most recent and precise are the estimates of Donnan et al. (2021): dt(AB) = 6.90 (+0.68/–0.69) d and dt(AC) = 9.43 (+0.83/–0.82) d. The lens galaxy is a part of a small group; the largest galaxy in the group is at about 25 arcsec to the South-West from the system. We measured positions of the group members using HST/WFC3 images (Fig. 1) and modeled these galaxies as point masses.

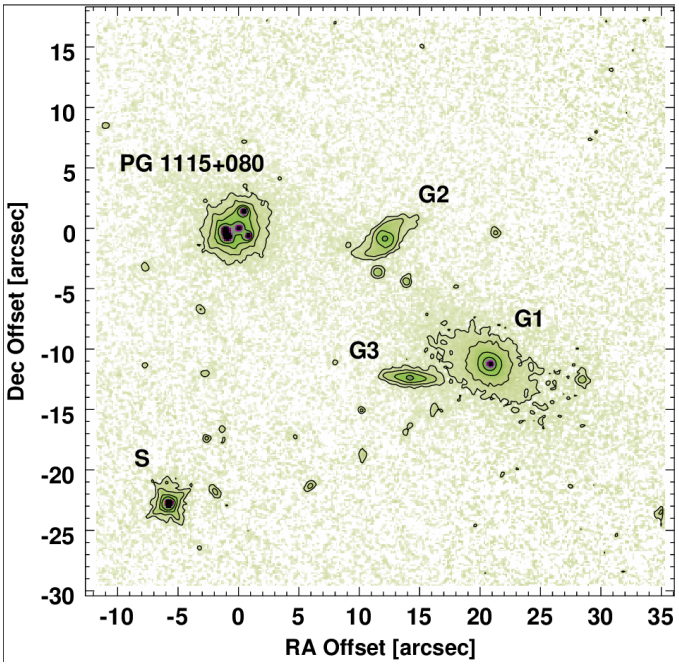

Fig. 1: *The galaxy group close to PG 1115+080 imaged by HST/WFC3.*

WFI 2033-4723. This quadruple system was discovered by Morgan et al. (2004). The lens redshift is z_L = 0.6575 (Sluse et al. 2019) and the source one is z_S = 1.66044 (Momcheva et al. 2015). The astrometry was taken from Vuissoz et al. (2008). The time delays between the BCD images obtained so far are in agreement with each other. Bonvin et al. (2019) were able to obtain separate light curves of A1 and A2 images that allowed them to measure the time delays not relative to the composite A (=A1+A2) image, but to the images A1 and A2 themselves, i.e., dt(A1B) and dt(A2C). Regarding dt(A1A2), there is some controversy: Morgan et al. (2018) claimed that A1 leads A2 by 3.9 d, whereas Bonvin et al. (2019) found the opposite: A2 leads A1 by a day. We tested both options. In the case A2 leading A1, however, we

got an arrival-time surface with critical points in locations not occupied by the A1 and A2 images. So, we assume that A1 leads A2. We ran PixeLens twice. Initially, we set dt(A1A2) = 0 and as a result we estimated the A1A2 time delay of 3.0 (+0.7/–0.7) d at 68% confidence. Then we used the value of 3.9 d for the final run.

Based on the 100 mass models run, we build the mass steepness index distribution for each lens. The steepness index and its uncertainty for each lens was derived by means of Gaussian fitting (Fig. 2). The steepness index itself is defined as $\Sigma(R) \sim R^{-(\text{steepness index})}$, where Σ is the surface mass distribution. We got the following results: 0.64 ± 0.15 for DES J0408–5354, 0.97 ± 0.18 for PG 1115+080, and 0.93 ± 0.12 for WFI 2033–4723. So, the steepness index was found to be less than 2, i.e., the radial density profiles are shallower than R^{-2} and are consistent with isothermality. Finally, the mass and light distributions were found to be matched well in both orientation and ellipticity.

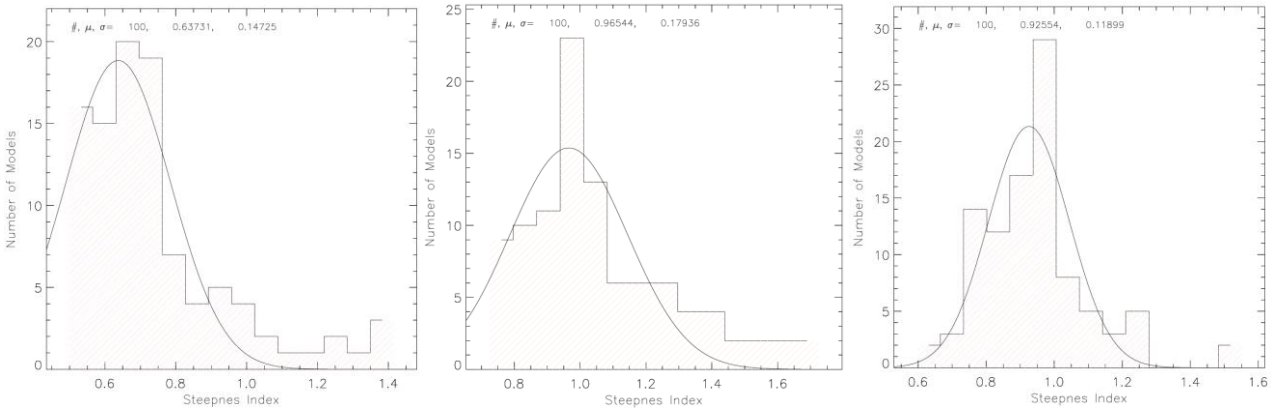

Fig. 2: *Steepnes index distributions for DES J0408–5354 (left), PG 1115+080 (middle), and WFI 2033–4723 (right). The fitted Gaussians, together with the number of runs and the Gaussian mean and sigma are listed in each plot.*

Acknowledgements and References

This research is based on activities partially supported by the Bulgarian National Science Fund under contract DN 18/13-12.12.2017.

Bonvin et al. 2019, A&A, 629, A97
Donnan, F. R., Horne, K., Hernández Santisteban, J. V. 2021, MNRAS, 508, 544
Lin et al. 2017, ApJL, 838, L15
Momcheva et al. 2015, ApJS, 219, 29
Morgan et al. 2004, AJ, 127, 2617
Morgan et al. 2008, ApJ, 689, 755
Morgan et al. 2018, ApJ, 869, 106
Peng et al. 2010, AJ, 139, 2097
Saha, P., Williams, L. L. R. 2004, ApJ, 127, 2604
Shajib et al., 2019, MNRAS, 483, 5649
Sluse et al. 2019, MNRAS, 490, 613
Tonry, J. L. 1998, AJ, 115, 1
Vuissoz et al. 2008, A&A, 488, 481
Weymann et al. 1980, Nature, 285, 641